A MODAL METHOD FOR TRANSIENT THERMAL ANALYSIS OF CANDU FUEL CHANNEL

JONG-WOON, PARK* AND AJIT P. MUZUMDAR**

* Institute for Advanced Engineering (IAE), Korea
** Visiting professor at IAE on attachment from AECL, Canada

ABSTRACT

The classical modal expansion technique has been applied to predict transient fuel and coolant temperatures under on-power conditions in a CANDU fuel channel. The temperature profile across the fuel pellet is assumed to be parabolic and fuel and coolant temperatures are expanded with Fourier series. The coefficient derivatives are written in state space form and solved by the Runge-Kutta method of fifth order. To validate the present model, the calculated fuel temperatures for several sample cases were compared with HOTSPOT-II, which employs a more rigorous finite-difference model. The agreement was found to be reasonable for the operational transients simulated. The advantage of the modal method is the fast computation speed for application to a real-time system such as the CANDU simulator which is being currently developed at the Institute for Advanced Engineering (IAE).

1. INTRODUCTION

A reliable thermo-hydraulic model for the nuclear reactor core must have the capability of calculating transient temperature distributions in fuel rods as accurately as possible under various conditions such as normal operation, operational upsets, and loss of coolant accidents. With respect to the CANDU nuclear power plant real-time simulator being developed at IAE, it is also required that the thermo-hydraulic conditions for a number of fuel channels should be calculated simultaneously as economically as possible for operational transients including reactor trip.

Compared to pressurized water reactors, in the pressure-tube-type CANDU reactor core, the coolant channels are separated from each other by pressure/calandria tubes (no channel-to-channel cross flow) so the axial flow is dominant. Owing to such an axial flow dominance, CANDU reactor core thermo-hydraulic analysis is usually performed separately for each channel or group of channels.

There have been a variety of models and numerical methods dealing with fuel-to-coolant transient heat transfer problems for the CANDU core. In the following, the major existing models will be briefly reviewed:

The HOTSPOT-II [1] code is a detailed fully implicit finite-difference two-dimensional cylindrical model of a CANDU fuel bundle, that has a lot more capability than is required for the real-time simulator. It is usually used as a slave tool for detailed information on fuel bundle and pressure tube/calandria tube temperatures and requires the heat generation rate and coolant boundary conditions as input parameters. The demerit of the method is that the finite difference scheme may be too time-consuming for the real time simulator model if temperatures in each fuel bundle are required.

The fuel model in system thermal-hydraulic codes such as SOPHT [2] is essentially an explicit 1-D version of the HOTSPOT single-pin model, usually employing only about 5 radial nodes in the fuel, gap, and sheath. It has been found to be fairly accurate based on studies comparing SOPHT versus HOTSPOT-II. Although the solution method is very straight-forward, numerical stability requirements imply that the explicit method may or may not be more time-consuming than the fully implicit method.

The fuel model in the CHAN code [3] is based on an electrical analogue. The equations are relatively simple, and probably very fast to solve as no exponents are involved. The problem is that the model was originally derived for decay heat conditions during LOCA scenarios, assuming a flat temperature distribution across the fuel pellet. It has been found[1] that the current CHAN model is fairly accurate for poor cooling conditions, under full or decay power, during which a fairly flat temperature gradient across the fuel is maintained.

The fuel model developed for use with the DSNP code [4] is based on the FUELPIN code [5], in which a lumped parameter approach is used. It is assumed that the coolant boundary conditions and heat transfer coefficient are obtained separately. However, this model has limitations for fast transients such as a

reactor trip.

The basic idea of the modal heat transfer model is that parameters such as the heat generated in the fuel, the fuel temperature, and the coolant temperature, can be represented as a Fourier series expansion. By writing the heat balance equations for the fuel and coolant, then substituting the Fourier series expansions, and finally integrating over the channel length, a series of linear differential equations can be obtained for the Fourier coefficients. The solution of these equations allows the fuel and coolant temperatures to be determined as a function of time. One of the advantages of this model is that it allows fuel and coolant temperatures for all axial locations in a channel to be determined simultaneously. Another useful aspect of the method is that, with appropriate modifications, it allows a calculation of the channel boiling length, the average channel quality, and the channel outlet quality. These are important for operational transients where fuel dryout and void reactivity may be important considerations.

The modal method, if properly modified and improved, appears very promising for operational transients. Carslaw and Jaeger [6] noted that the Fourier expansion method is completely adequate for problems in finite regions. In addition, since this method produces fuel and coolant temperatures for an entire channel simultaneously, it may be very economical to use for a three dimensional CANDU reactor core thermo-hydraulic model within the real-time engineering simulator model.

The modal fuel channel heat transfer model was developed for the Bruce A CANDU nuclear training simulator [7]. However, the major limitation of the original modal method is that it assumes that the sheath temperature is always equal to the fuel average temperature, which may not be adequate for the present purpose. In this paper, therefore, the existing modal analysis method has been extended to account for the temperature distribution in the fuel, gap, and sheath. Simplified analysis has been carried out neglecting circumferential temperature variations, and the fuel temperature profiles obtained are compared with HOTSPOT-II code predictions.

2. ANALYTICAL MODEL

2.1 Governing Energy Balance Equations

The governing heat balance equations for the radially averaged fuel temperature and coolant temperatures for the CANDU fuel pin and channel geometry shown in Fig. 1 can be formulated from an energy balance on an elementary length of the fuel channel using the following basic assumptions:

(1) No boiling;
(2) Negligible axial heat conduction;
(3) Parabolic temperature profile across the fuel pellet [the fuel element is in the thermally thin conduction regime (see Ref. 8)];
(4) No circumferential temperature variations;
(5) Constant thermo-physical properties;
(6) Radially uniform volumetric heat generation rate;
(7) Negligible heat transfer to the moderator; and
(8) Negligible thermal inertia of fuel sheath compared to the fuel pellet.

Writing an energy balance and rearranging gives:

$$\frac{\partial T_F(t,z)}{\partial t} = \frac{q'''(t,z)}{\rho_F c_{pF}} + [T_C(t,z) - T_S(t,z)]\frac{hS_S}{\rho_F c_{pF} A_F} \tag{1}$$

$$\frac{\partial T_C(t,z)}{\partial t} + V\frac{\partial T_C(t,z)}{\partial z} = [T_S(t,z) - T_C(t,z)]\frac{hS_S}{\rho_C c_{pC} A_S} \tag{2}$$

where T is the temperature, t is the time, q''' is the volumetric heat generation rate in fuel, ρ is the average density, c_p is the specific heat capacity, h is the onvective heat transfer coefficient from sheath to coolant, V is the coolant velocity, and the subscrips F, C, and S denote fuel average, coolant, and sheath outer surface, respectively.

The assumption that the temperature profile across the fuel pellet has a parabolic shape gives the following equation for the average fuel temperature (from here (t,z) will be left out for temperatures):

$$T_F = \frac{1}{2}(T_{CL} + T_{Fo}) \tag{3}$$

where T_{CL} and T_{Fo} are the fuel centerline and fuel outer surface temperatures, respectively.

Equation (3) is a key assumption which simplifies the derivation of the energy equation. Note that the average fuel temperature T_F is identical to the temperature at approximately 70% of the fuel radius for a parabolic profile.

Assuming the fuel sheath has negligible thermal inertia compared to the fuel pellet, we can equate the total heat loss from the fuel surface to the instantaneous heat conducted across the fuel pellet to obtain:

$$h(T_S - T_C)\frac{r_S}{2} = k_F(T_{CL} - T_{Fo}) \tag{4}$$

where r_S is the fuel sheath outer surface radius and k_F is the thermal conductivity of the fuel pellet.

Similarly, relating the instantaneous heat flux across the fuel-sheath gap to the heat flux to the coolant, we obtain:

$$h_g(T_{Fo} - T_{Si}) = \frac{r_S}{r_F} h\,(T_S - T_C) \tag{5}$$

where h_g is the heat transfer coefficient through the gap and r_F is the fuel pellet outer surface radius.

After eliminating T_{Fo} from Eqs.(4) and (5), we obtain the following equation for T_S:

$$T_S = T_C + \frac{1}{\frac{hr_S}{4k_F} + \frac{hr_S}{h_g r_F}} T_F - \frac{1}{\frac{hr_S}{4k_F} + \frac{hr_S}{h_g r_F}} T_{Si} \tag{6}$$

Equating the heat flux across the fuel sheath thickness δ_{cl} to the convective heat transfer to the coolant gives the following equation for the sheath inner temperature:

$$T_{Si} = T_S + \frac{h\delta_{cl}}{k_{cl}}(T_S - T_C) \tag{7}$$

Substituting Eq.(7) into Eq.(6), we obtain:

$$T_S = (1 - h^*)\,T_C + h^*\,T_F \tag{8}$$

where the dimensionless parameter h^* is defined by

$$h^* = \frac{1}{\frac{hr_S}{4k_F} + \frac{hr_S}{h_g r_F} + \frac{h\delta_{cl}}{k_{cl}}} \tag{9}$$

We now define the following time constants:

$$\tau_F = \frac{\rho_F c_{pF} A_F}{hS_S h^*} \tag{10a}$$

$$\tau_C = \frac{\rho_C c_{pC} A_S}{hS_S h^*} \tag{10b}$$

where τ_F is the fuel time constant and τ_C is the corresponding coolant time constant.

Substituting Eq.(8) into Eqs.(1) and (2), we obtain

$$\frac{\partial T_F(t,z)}{\partial t} = \frac{q'''(t,z)}{\rho_F c_{pF}} + \frac{T_C(t,z) - T_F(t,z)}{\tau_F} \tag{11a}$$

$$\frac{\partial T_C(t,z)}{\partial t} = \frac{T_F(t,z) - T_C(t,z)}{\tau_C} - V\frac{\partial T_C(t,z)}{\partial z} \tag{11b}$$

The fuel and coolant temperatures, and heat generation rate can be expanded in Fourier series with coefficients $a_{Fn}(t)$, $b_{Fn}(t)$, $a_{Cn}(t)$, $b_{Cn}(t)$ and $C_n(t)$, respectively over the period $2L$ (from $-L$ to L) where L is the channel length as follows:

$$T_F(t,z) = a_{Fo}(t) + \sum_{n=1}^{N}\left[a_{Fn}(t)\cos(\frac{n\pi z}{L}) + b_{Fn}(t)\sin(\frac{n\pi z}{L})\right] \tag{12a}$$

$$T_C(t,z) = a_{Co}(t) + \sum_{n=1}^{N}\left[a_{Cn}(t)\cos(\frac{n\pi z}{L}) + b_{Cn}(t)\sin(\frac{n\pi z}{L})\right] \tag{12b}$$

$$q'''(z,t) = \sum_{n=1}^{N} C_1(t)\ \sin(\frac{n\pi z}{L}) \tag{13}$$

$$C_n(t) = \frac{2}{L}\int_0^L q'''(z,t)\sin(\frac{n\pi z}{L})\,dz \tag{14}$$

where an axially symmetric heat generation is assumed for simplicity, although an expansion in terms of sines and cosines could easily be implemented for more general cases.

Substituting the above equations into Eqs.(11a) and (11b), integrating from $-L$ to L gives the following time derivatives for the Fourier coefficients a_{Fo} and a_{Co} respectively:

$$\frac{d}{dt}a_{Fo}(t) = \frac{1}{\tau_F}\ [\ a_{Co}(t) - a_{Fo}(t)\ ] \tag{15a}$$

$$\frac{d}{dt}a_{Co}(t) = \frac{1}{\tau_C}\ [\ a_{Fo}(t) - a_{Co}(t)\ ] \tag{15b}$$

Substituting Eqs.(12a) through (13) into Eqs.(11a) and (11b), integrating from $-L$ to after multiplying by $cos(n\pi z/L)$ gives the following time derivatives for the Fourier coefficients a_{Fn} and a_{Cn} $(n=1, 2, \ldots, N)$, respectively:

$$\frac{d}{dt}a_{Fn}(t) = \frac{1}{\tau_F}\ [\ a_{Cn}(t) - a_{Fn}(t)\ ] \tag{15c}$$

$$\frac{d}{dt}a_{Cn}(t) = \frac{1}{\tau_C}\ [\ a_{Fn}(t) - a_{Cn}(t)\ ] - \frac{n\pi V}{L}b_{Cn}(t) \tag{15d}$$

Repeating this procedure, but integrating from $-L$ to L after multiplying by $sin(n\pi z/L)$ gives the following time derivatives for the Fourier coefficients b_{Fn} and b_{Cn}, respectively:

$$\frac{d}{dt}b_{Fn}(t) = \frac{C_n(t)}{\rho_F c_{pF}} + \frac{1}{\tau_F}\ [\ b_{Cn}(t) - b_{Fn}(t)\ ] \tag{15e}$$

$$\frac{d}{dt}b_{Cn}(t) = \frac{1}{\tau_C}\ [\ b_{Fn}(t) - b_{Cn}(t)\ ] + \frac{n\pi V}{L}a_{Cn}(t) \tag{15f}$$

2.2 Steady State Equations

Substituting $z = 0$ in Eq.(12b), the following channel inlet boundary condition is obtained:

$$T_{C,i}(t) = a_{Co}(t) + \sum_{n=1}^{N} a_{Cn}(t) \tag{16}$$

The steady state solution for any channel power state, i.e., initial conditions for the Fourier coefficients, can be obtained by equating the time derivatives of Eq.(15) to zero to obtain:

$$a_{Fo}(0) = a_{Co}(0) = T_{C,i}(0) + \sum_{n=1}^{N}\left(\frac{\tau_F C_n(0)/\rho_F c_{pF}}{\tau_C \pi V/L}\right) \tag{17a}$$

$$a_{Fn}(0) = a_{Cn}(0) = -\left(\frac{\tau_F C_n(0)/\rho_F c_{pF}}{\tau_C \pi V/L}\right) \tag{17b}$$

$$b_{Fn}(0) = \frac{\tau_F C_n(0)}{\rho_F c_{pF}} \tag{17c}$$

$$b_{Cn}(0) = 0 \tag{17d}$$

where $T_{C,i}(0)$ is the initial inlet temperature.

2.3 Transient Equations

When Eq.(16) is also substituted into Eqs.(15a) and (15b) to eliminate a_{Co}, we obtain:

$$\frac{d}{dt}a_{Fo}(t) = \frac{1}{\tau_F}\left[\, T_{C,i}(t) - a_{C1}(t) - a_{C2}(t) - a_{C3}(t) - a_{Fo}(t) \,\right] \tag{15g}$$

$$\frac{d}{dt}a_{Co}(t) = \frac{1}{\tau_C}\left[\, T_{C,i}(t) - a_{F1}(t) - a_{F2}(t) - a_{F3}(t) - a_{Co}(t) \,\right] \tag{15h}$$

Equations (15g) and (15h) together with Eqs.(15c) through (15f) sholud be solved to obtain the Fourier coefficients as a function of time. Substitution of the Fourier coefficients into Eq.(12) allows the fuel and coolant temperatures to be determined at any axial location as a function of time.

Considering only the first 4 Fourier Terms in Eq.(12), i.e., $N = 3$, the system of equations for the Fourier coefficients, a_{Fo}, a_{Fn}, b_{Fn}, a_{Co}, a_{Cn}, and b_{Cn} ($n=1, 2, 3$), can be arranged in the following form:

$$\dot{x}(t) = Ax(t) + Bu(t) \tag{18}$$

where A and B are the coefficient matrices and $x(t)$ is the solution vector given by

$$x = [\, a_{Fo}(t)\ a_{F1}(t)\ b_{F1}(t)\ \ldots\ a_{F3}(t)\ b_{F3}(t)\ a_{Co}(t)\ a_{C1}(t)\ b_{C1}(t)\ \ldots\ a_{C3}(t)\ b_{C3}(t)\ ]^T \tag{19}$$

and the input vector $u(t)$ is

$$u(t) = [\, C_1(t)\quad C_2(t)\quad C_3(t)\quad T_{C,i}(t)\ ]^T \tag{20}$$

The matrices A and B in Eq.(18) can be simply constructed by using Eqs.(15c)-(15h), and therefore, they are not presented here. Note that, in principle, any number of Fourier terms may be considered using this method. Equation (18) can be referred to as a state-space model in control theory and can be easily solved by using MATLAB-Simulink [8], a commercial scientific calculation software package mostly used in solving linearly time invariant (LTI) state-space models in control engineering. In the present paper the model building has been done using the built-in graphical user interface which makes the programming very quick and convenient. This commercial tool has been used mostly in order to provide a high assurance of accuracy and to avoid time-consuming programming work. FIG. 2 shows the Simulink model that is constructed which consists of the present state space model matrices A and B, and functions for the calculation of temperatures at other radial positions. The solution method used here is the well-known Runge-Kutta method of fifth order and variable time mesh.

For verification of the present model by comparing it with the results of the HOTSPOT-II computer code, the following procedure has been used:

(1) Initialize the Fourier coefficients of the modal equations,
(2) Calculate the fuel and coolant temperatures using the modal equations,
(3) Input history of thermal power and coolant temperatures at any axial location from the modal method into HOTSPOT-II,
(4) Calculate the transient temperature distributions in the fuel, gap and sheath

regions using HOTSPOT-II, and
(5) Compare the fuel centerline and fuel average temperatures from the two models.

3. RESULTS AND DISCUSSION

The steady state radial temperature profiles calculated by the present model and HOTSPOT-II at the axial center of the channel are shown in FIG. 3. Typical simulation parameters used are shown in TABLE 1. The data presented in TABLE 1 corresponds to nominal full power data for 600 MWe CANDU nuclear power plants. The simulated fuel element is that in the outer ring of a 37-element fuel bundle. The agreement is seen to be excellent in FIG. 3.

Figure 4 shows the calculated initial axial profile of the fuel average and coolant temperatures using the modal method, and the profile of the initial axial heat generation distribution in the steady-state prior to the transient simulation.

In order to compare the present method with HOTSPOT-II results, the following three transient cases are simulated using the two methods on an IBM personal computer 486DX2/66MHz:

(1) Step increase in heat generation from 100% to 110%,
(2) Linear reduction from 100% to decay heat level (7%) in 10 seconds (i.e., rate of -9.3%/sec), and
(3) Channel inlet temperature increase from 266.5 °C to 276.5 °C in 100 seconds (i.e., rate of 0.1 °C/sec).

The thermo-physical properties, such as density, specific heat, flow velocity, and heat transfer coefficients are held constant throughout the transient and a simple cosine power distribution about the axial center with $C_1 = 4.661 \times 10^8$ W/m^3 $C_2 = C_3 = 0$ is assumed. In this case, a_{Fn}, b_{Fn}, a_{Cn}, b_{Cn} with n greater than 1 are all zeros.

A variable time-step size ranging from 0.001 to 0.1 second is used for the present modal method, whereas, in HOTSPOT-II, a fixed standard time-step size of 0.05 second has been used. However, the same convergence criterion, i.e., 1×10^{-6}, has been used for the two methods. The standard recommended number of radial nodes in the fuel (6 nodes), sheath (3 nodes), and gap (1 node) has been used.

3.1 Case (1)

For the first case of a step increase in fuel heat generation rate from 100% full power to 110% full power at 20 seconds, the fuel centerline and average temperature responses at the center of the channel (z = L/2) calculated by the present model and HOTSPOT-II, the coolant temperature calculated by the present method, and the input curve of volumetric heat generation rate are shown in FIG. 5. In the case of the fuel centerline temperature, the agreement is fairly good except that the temperature calculated by the present method is a little higher than HOTSPOT-II during the transient period. This is due to the fact that the present method assumes a radially parabolic temperature profile in the fuel region as in Eq.(3). Therefore, the fuel centerline temperature changes with the same characteristic time as τ_F of the fuel average temperature. However, in HOTSPOT-II the characteristic time will be different for the different radial fuel regions because it solves the finite-difference conduction equation accurately.

In the case of the fuel average temperature, the apparent difference between the present method and HOTSPOT-II is due to the nodal averaging method in HOTSPOT-II, where no account is taken of the temperature profile through a radial fuel node. In actual fact, the rates of change of the two curves are still very close to each other and the time constants are nearly the same.

Figure 6 shows the Fourier coefficients versus time in this case. The oscillatory behavior of b_{C1} can be explained as follows: a fast increase in C_1 results in a fast increase of b_{F1} in Eq.(15e), which gives a fast increase in time derivative of b_{C1} at the current time step due to the positive sign of b_{F1} in Eq.(15f). This tends to increase the absolute value of a_{C1} (a_{C1} is negative as shown in FIG. 6) according to Eq.(15d). At the next time step, this tends to decrease the value of b_{C1} according to the positive sign of a_{C1} in Eq.(15f), which will increase a_{C1} according to Eq.(15d). However, the amplitude of oscillation of b_{C1} is very small.

3.2 Case (2)

The second case simulated is a fast reduction in fuel heat generation rate (such as a reactor trip) from 100% full power to decay heat level (about 7% full power) in 10 seconds. The time variation of the heat generation rate is shown at the bottom of FIG. 7. The fuel centerline temperature curves at z = L/2 calculated by the present model and HOTSPOT-II are very close to each other. The speed of the

temperature change is also slightly faster in the modal model, due to the same reasons as given previously. The small difference between the two curves of fuel average temperatures from the present model and HOTSPOT-II is also largely due to the nodal averaging method used in HOTSPOT-II.

The agreement between the two sample cases above shows that the assumption of a radially parabolic temperature profile in the fuel throughout the transient is a reasonable assumption even for fast transients resulting from rapid power changes.

3.3 Case (3)

Figure 8 shows the calculated fuel centerline temperature versus time at z = L/2 for an inlet temperature variation from 266.5 °C to 276.5 °C in 100 seconds. It is seen that the fuel centerline temperature calculated by the present model rises slightly faster than in HOTSPOT-II. However, the difference between the two methods is less than 2 °C. The difference in fuel average temperatures is again largely due to the nodal averaging in HOTSPOT-II.

The CPU times which have been obtained during the sample runs for the first case (simulation time is 100 seconds) using the present method and HOTSPOT-II are about 2 seconds and 19 seconds, respectively. Considering that a part of the CPU time taken by the present model has been spent for the calculation of coolant temperatures, it can be seen that the present modal method is much faster and more efficient than a detailed finite-difference conduction model. Furthermore, the modal method can easily provide fuel and coolant temperatures simultaneously for the entire channel as an analytical expression given by Eq.(12), whereas the detailed finite difference model has to be run at each axial location specified. For example, if fuel temperatures are needed at each of the 13 bundle locations, the CPU time per fuel channel would be reduced by a factor of approximately 260 using the modal method.

3.4 Test for Two-Phase Application

In order to test the applicability of the present model to the case when the coolant in the fuel channel is two-phase, the channel is subdivided into subcooled region upstream of the boiling boundary and two-phase (saturated) region downstream. The time dependednt axial temperature profile of subcooled coolant is calculated by the present model, and the coolant downstream of the boiling boundary is assumed to have a fixed saturation temperature, which, therefore, becomes the channel outlet temperature.

The test run for the reactor trip case for Wolsung 3&4 is compared with the results of SOPHT [9]. The time history of the channel inlet end fitting temperature calculated by SOPHT is used as a boundary condition of the present model, i.e., $T_{C,i}(t)$ in Eq.(20). The coolant velocity used (V = 10 m/sec) is an average of the typical values for the single-phase and two-phase conditions in the CANDU 6 fuel channel. The value of fuel-to-coolant heat transfer coefficeint is different from that listed in TABLE 1 since the coolant condition should be two-phase, and the volumetric heat generation rate is increased to 5.732×10^8 W m^{-3} to obatain outlet quality of 1.74%.

Results of the simulation is shown in FIG. 9. It shows that the coolant temperature at the channel outlet end fitting calculated by present model is close to but somewhat slower than the result of SOPHT [9]. This is because the present model does not consider system pressure (i.e., saturation temperature) drop in the trip condition. And although the assumption of constant heat transfer coefficient may be a crude one, FIG. 9 shows that this assumption is justifiable in that we are mainly interested in the channel outlet condition.

4. CONCLUSION

The classical modal expansion technique has been modified to predict transient fuel and coolant temperatures for a number of sample cases. After comparing the present method with a more detailed code such as HOTSPOT-II for three cases such as a step increase in thermal power, a fast reduction in thermal power, and an inlet temperature ramp, it has been verified that the present modal method is reasonably accurate and the calculation speed is significantly improved for operational type transients.

Note that the assumption of constant thermo-physical parameters in the present method can be easily relaxed by modifying the present linearly time invariant matrices, A, B, and u in the present state space equations and feeding back the updated values of thermo-physical parameters such as density, specific heat,

flow velocity, and heat transfer coefficients. The condition when the coolant is two-phase has been considered by replacing the present model with a two-region model where the upstream subcooled region is solved by the present model, and the downstream region is at a fixed coolant temperature, i.e., saturation temperature.

REFERENCES

(1) MUZUMDAR, A.P., SAKAGUCHI, R.L., and PRESELY, J.K., "HOTSPOT-II Fuel Bundle Thermal Response Code", Nuclear Studies and Safety Department, Report No. 83058, April, 1983.

(2) CHANG, Y.F. and SKEARS, J., "A Thermal-Hydraulic System Simulation Model for Reactor, Boiler and Heat Transport System (SOPHT)", Ontario Hydro, Central Nuclear Services Report No CNS-37-2, 1977.

(3) GILLESPIE, G.E., HARRISON, W.C., HILDERBRANDT, J.G., and LEDOUX, G.A., "Thermal Behavior of a CANDU-PHW Reactor Fuel Channel Containing Nearly Superheat Steam," Proc. of Int. Meeting on Thermal Nuclear Reactor Safety, Chicago, 1982.

(4) SAPHIER, D. "The Level-One Modules Library for DSNP: Dynamic Simulator for Nuclear Power Plants," Technical Memorandum, ANL-CT-77-22 Rev. EBR-3.5, Canadian Edition, edited and revised by Pitre, J., UNB, 1992.

(5) RANCE, F. "FUELPIN - Fuel Temperature Simulation Code User's Guide," Ontario Hydro Report No. 82034, 1969.

(6) CARSLAW, H.S. and JAEGER, J.C., "Conduction of heat solids", Oxford University Press, Oxford, 1959.

(7) Ontario Hydro, private communication from Kwan, D. to Muzumdar, A.P.

(8) MATLAB-Simulink, the Math Works Inc., 1992.

(9) Transient Analysis Report, Wolsung 3&4.

TABLE I. GEOMETRICAL AND THERMOPHYSICAL PARAMETERS USED

Parameter	Value	Unit
c_{pC}	5974.3	W/kg-°C
c_{pF}	0.317×10^{3}	W/kg-°C
D_F	12.154×10^{-3}	m
D_S	13.081×10^{-3}	m
h	31080	W/m^2-°C
h_g	10000	W/m^2-°C
k_{cl}	20	W/m-°C
k_F	3.2	W/m-°C
L	5.94	m
q_{max}	4.661×10^{8}	W/m^3
V	9.49	m/sec
δ_g	0.0445×10^{-3}	m
δ_{cl}	0.419×10^{-3}	m
ρ_C	737	kg/m^3
ρ_F	10.6×10^{3}	kg/m^3
τ_C	9.692	sec
τ_F	6.372	sec

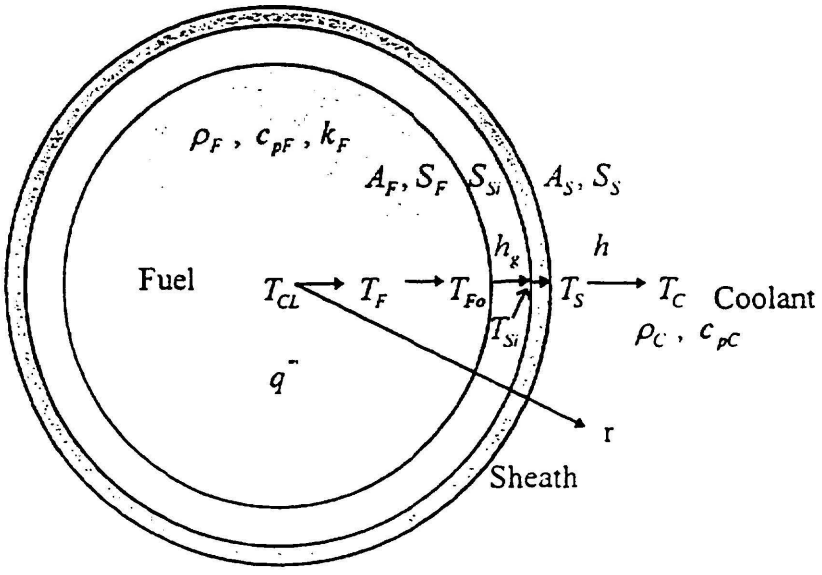

(a) CROSS-SECTIONAL VIEW OF FUEL SHEATH

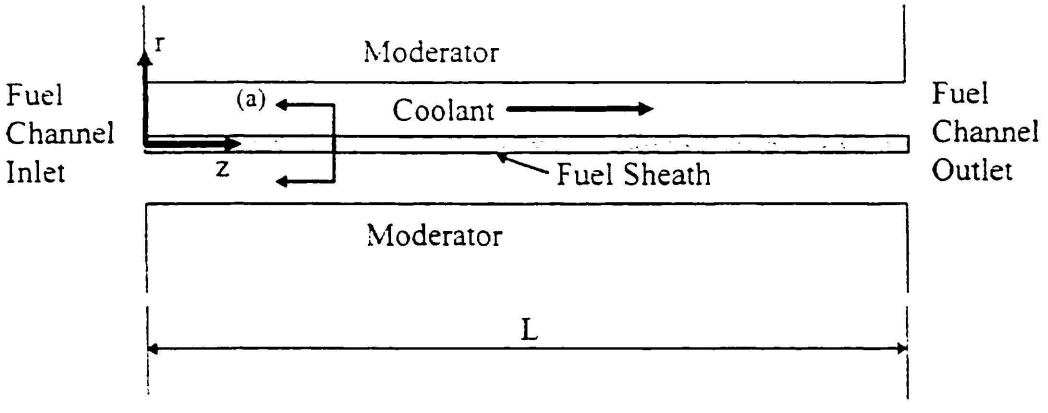

(b) AXIAL VIEW OF FUEL CHANNEL

FIG. 1. CANDU 6 FUEL PIN AND FUEL CHANNEL

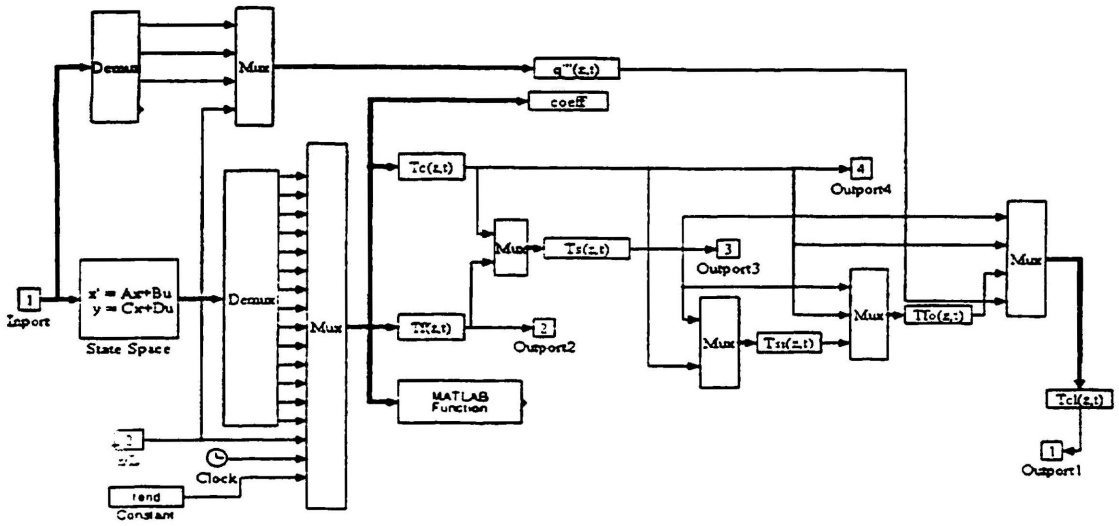

FIG. 2. MATLAB-SIMULINK™ MODEL

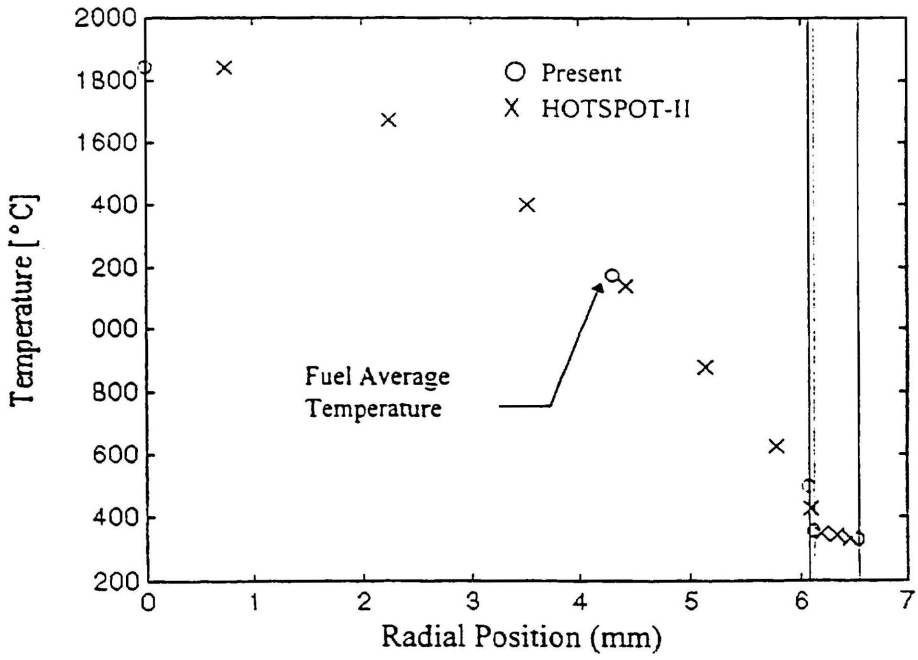

FIG. 3. STEADY STATE RADIAL TEMPERATURE PROFILE CALCULATED BY PRESENT MODEL AND HOTSPOT-II

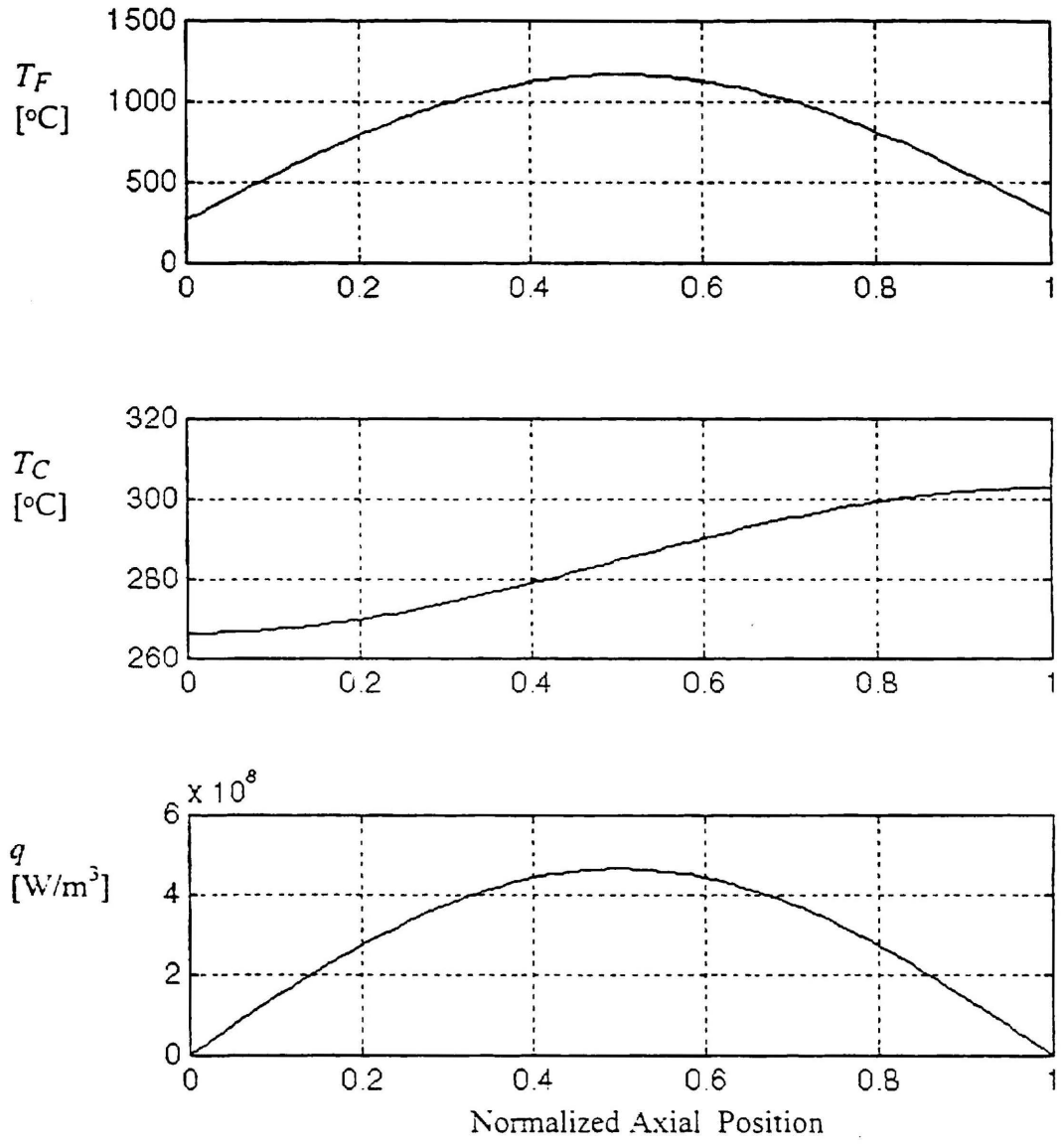

FIG. 4. STEADY STATE AXIAL TEMPERATURE AND HEAT GENERATION PROFILES

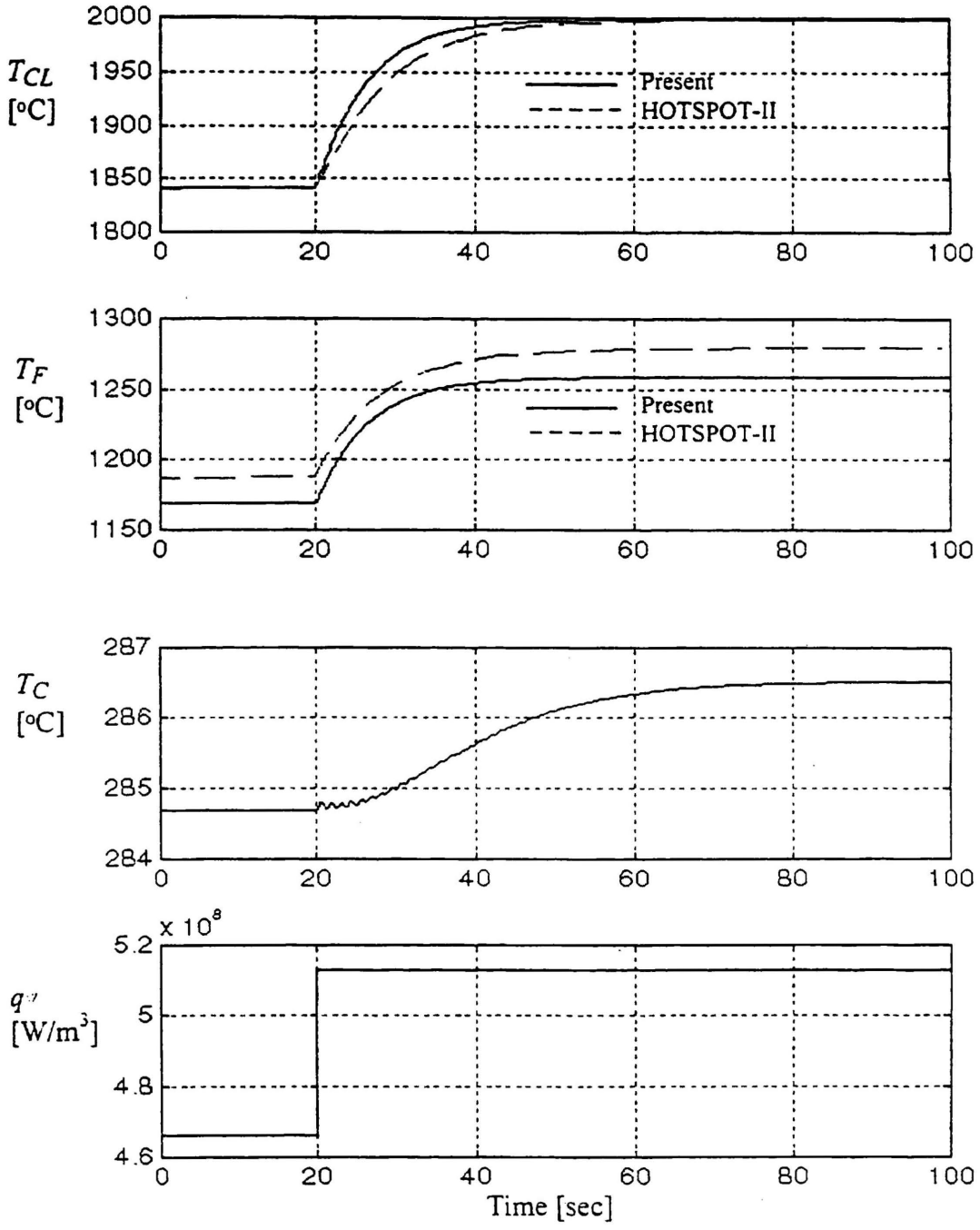

FIG. 5. FUEL CENTERLINE, AVERAGE, AND COOLANT TEMPERATURES AT Z = 0.5 L FOR 10% STEP INCREASE IN HEAT GENERATION RATE FROM 100% FULL POWER AS SHOWN AT THE BOTTOM OF THE FIGURE - CASE (1)

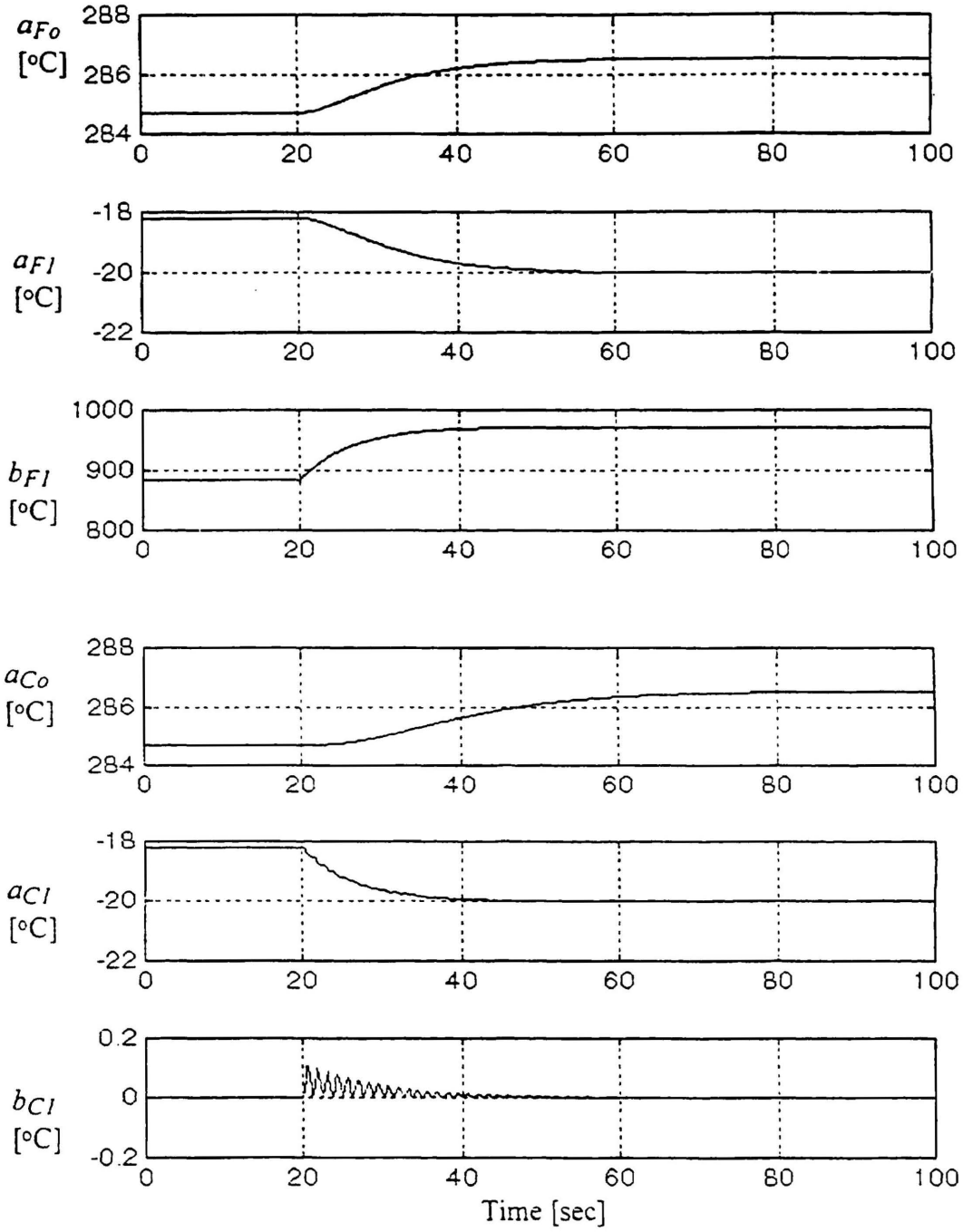

FIG. 6. VARIATION OF FOURIER COEFFICIENTS FOR 10% STEP INCREASE IN HEAT GENERATION FROM 100% FULL POWER - CASE (1)

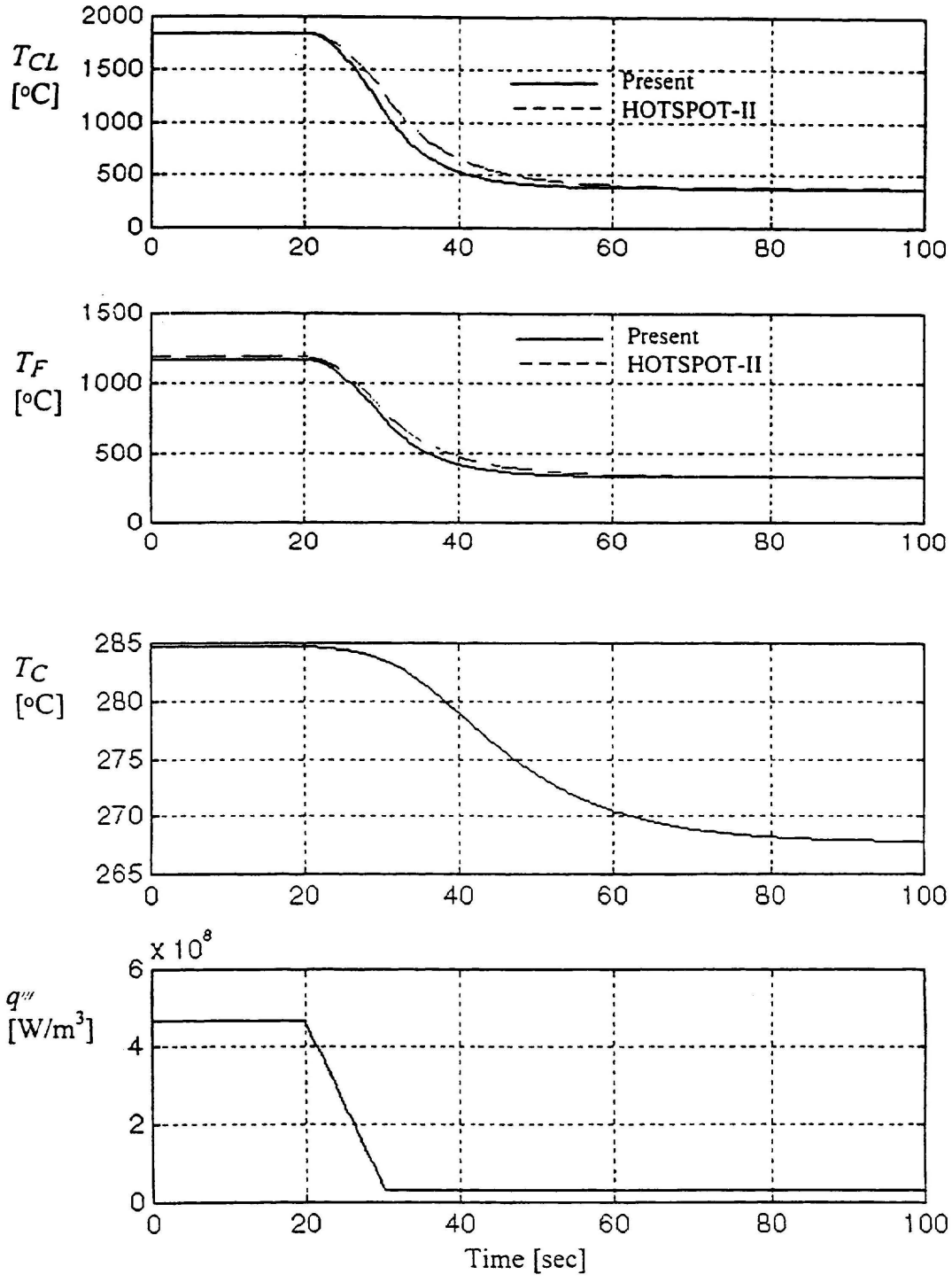

FIG. 7. FUEL CENTERLINE, AVERAGE, AND COOLANT TEMPERATURES AT Z = 0.5L FOR FAST REDUCTION OF HEAT GENERATION RATE FROM 100% FULL POWER TO DECAY HEAT LEVEL (7% FULL POWER) AT A RATE OF -9.3% AS SHOWN AT THE BOTTOM OF THE FIGURE - CASE (2)

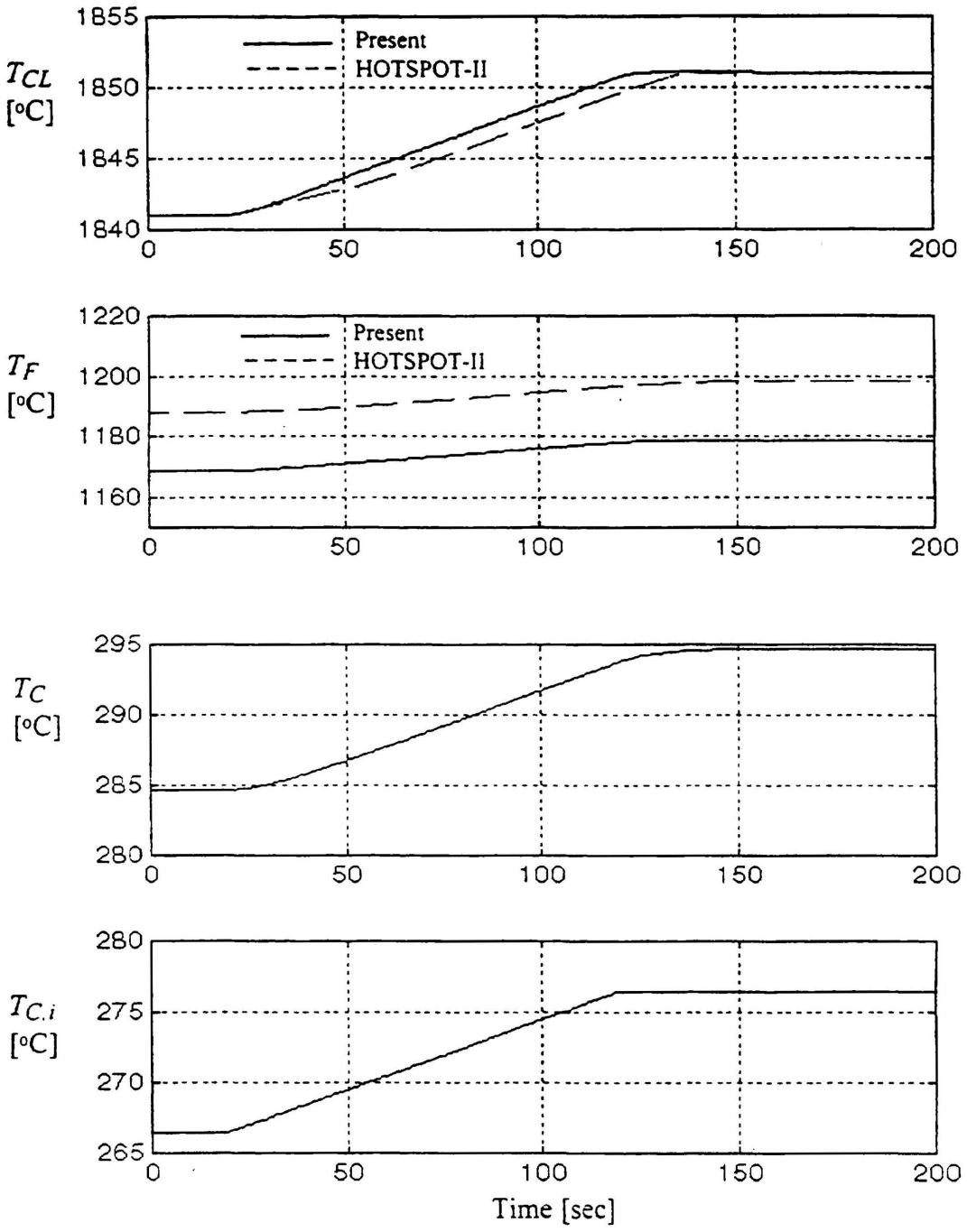

FIG. 8. VARIATION OF FUEL CENTERLINE, AVERAGE, AND COOLANT TEMPERATURES AT Z=0.5L FOR RAMP INCREASE OF TEMPERATURE AT THE CHANNEL INLET (Z=0) FROM 266.5 °C TO 276.5 °C IN 100 SECONDS - CASE (3)

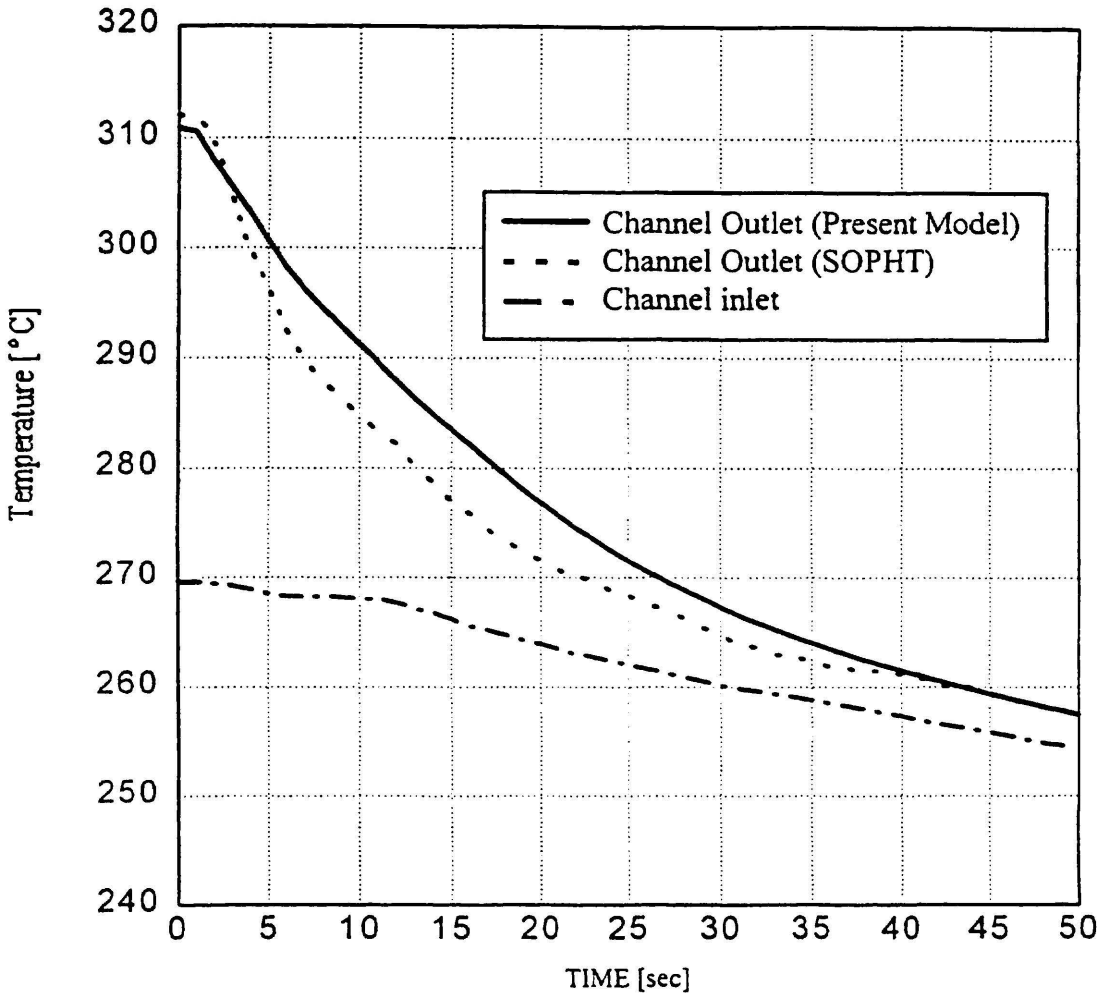

FIG. 9. COMPARISION OF CHANNEL OUTLET END FITIING TEMPERATURES BETWEEN PRESENT MODEL AND SOPHT SIMULATION FOR REACTOR TRIP (V = 10 m/sec , $\bar{q}_{max}$ = 5.732 x 10^8 W/m^3, h = 35314 W/m^2-°C, AND OTHER PARAMETERS ARE THE SAME AS LISTED IN TABLE 1)